

## **LabVIEW Based Transient Stability Analysis of A Multi-Machine System When Equipped With Hybrid Power Flow Controller**

Lini Mathew<sup>1</sup>, S.Chatterji<sup>2</sup>

<sup>1</sup>Associate Professor, NITTTR, Chandigarh.

<sup>2</sup>Professor, NITTTR, Chandigarh.

---

*Abstract - The high cost of the Voltage Source Converters (VSC) based FACTS controllers such as STATCOM, SSSC and UPFC is found to be the major hindrance to their widespread use. The classical controllers such as SVC and TCSC are important because of their simple construction, ease of use and low installation cost. Over the years, environmental, right-of-way and cost problems have delayed construction of generation facilities as well as new transmission lines. Better utilization of existing power systems and control equipment has thus become imperative. Novel and cost effective FACTS topologies therefore, need to be built upon existing equipment which makes use of static converters. The control performance of such topologies therefore, needs to be analyzed. Such controllers have been envisaged to be Hybrid Power Flow Controllers (HPFC). In the present work, the authors have made an attempt to simulate HPFC in terms of transfer function models. This simulated model has been tested by incorporating it in a Multi- Machine system. LabVIEW software has been employed for this purpose. Results obtained are encouraging and indicate that the dynamic performance of the power system has quite a bit improved with the HPFC.*

**Keywords – SVC, TCSC, SSSC, STATCOM, HPFC, Multi- Machine system**

---

### **I. INTRODUCTION**

The considerable price of VSC based FACTS Controllers, such as STATCOM, SSSC, UPFC etc, remain as the major impediment to their widespread use. The existing classical equipment such as switched capacitors and SVC used for voltage support and switched series capacitors and TCSC used for line impedance control have to be replaced whenever system upgrades or performance improvements are planned. These compensators are installed in many applications, in order to mitigate critical contingency conditions and while improvements in their performance would be worth considering, and their complete replacement is prohibitive. Several distinct models such as transfer function models have been proposed to represent SVC, TCSC, SSSC and STATCOM [1-8]. Concept of Hybrid Power Flow Controller (HPFC) has been proposed by Bebic et al. [9,10] but no model has been simulated so far and no stability studies carried out till date.

### **II. HYBRID POWER FLOW CONTROLLER**

The Hybrid Power Flow Controller (HPFC) employs two equally rated series connected voltage sourced converters to upgrade the functionality of the existing switched capacitors or Static VAR Compensators (SVC). Since, static converters are used together with passive devices the power flow controller can be considered as a hybrid controller, and is therefore named Hybrid Power Flow Controller (HPFC). The functions of switched capacitors and the SVC can be changed from reactive power support to the generalized power flow control by making use of appropriate converter control – the functionality commonly associated with UPFC. The key benefit of the new topology is that it fully utilizes the existing equipment and thereby the required ratings of the additional converters are substantially lower as compared to the ratings of the comparable UPFC [9].

The converters can exchange active power through a common dc circuit. A block diagram view of the envisioned typical HPFC controller is shown in Figure 1. The HPFC configuration is installed on a transmission line that connects two electrical areas on a Single Machine Infinite Bus (SMIB) System. Central to the HPFC topology is the shunt connected source of reactive power denoted by  $B_M$  and represents the controllable shunt connected variable capacitance. This is equivalent to a typical SVC or any other functional equivalents of SVC such as STATCOM, a synchronous condenser or even a mechanically switched capacitor bank. The two voltage sourced converters  $VSC_x$  and  $VSC_y$ , are connected to the transmission line by means of coupling transformers. The converters provide controllable voltages at the terminals of the high voltage side of the transformers. The converters share a common dc circuit coupling each others' dc terminals. The dc circuit permits exchange of active power between the converters [10]. HPFC can thus be regarded as the functional equivalent of UPFC.

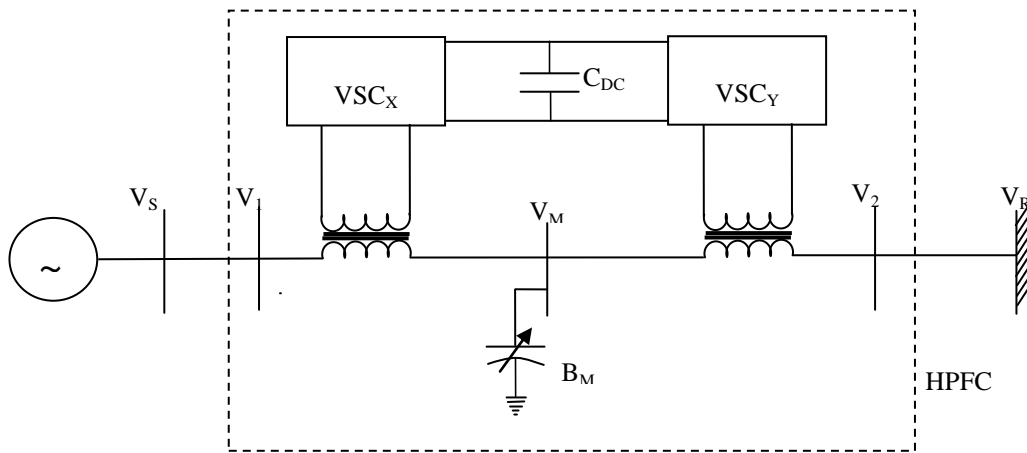


Fig.1. SMIB Power System Equipped with an HPFC

Two novel hybrid power flow controller (HPFC) topologies were proposed recently for FACTS. The first one consists of a shunt connected controllable source of reactive power, and the two series connected voltage sourced converters – one on each side of the shunt device. A simplified single-phase equivalent of the circuit corresponding to Fig.1 is shown in Fig.2.

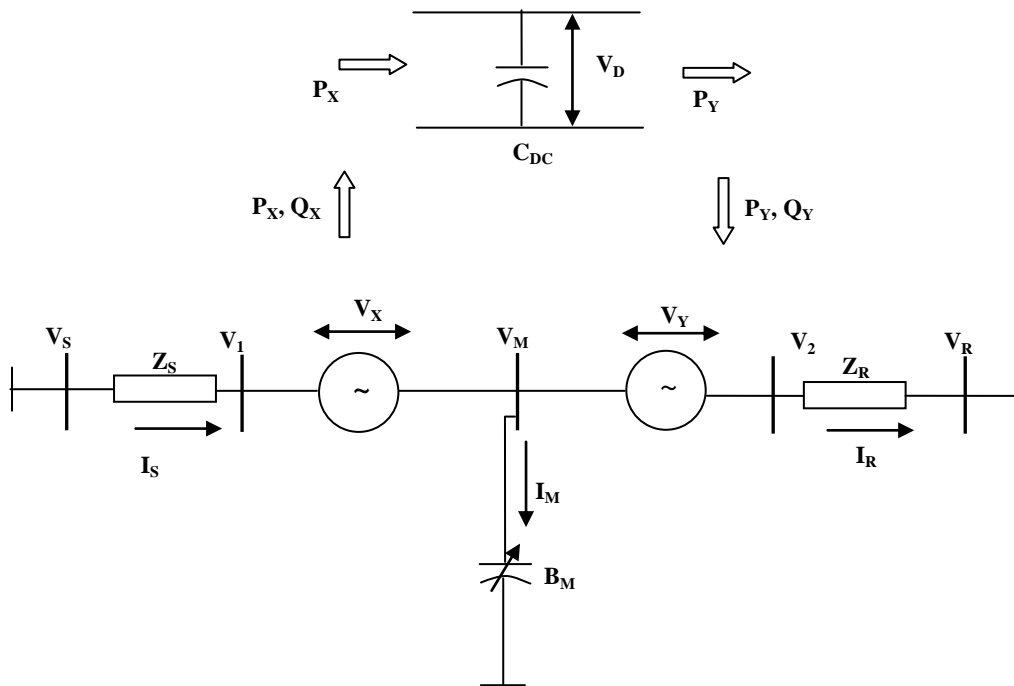


Fig.2 Simplified Single-Phase Equivalent Circuit of the System

The flow of active power through the line and the amounts of reactive power supplied to each line segment can be simultaneously and independently controlled by controlling the magnitudes and angles of voltages supplied by the converters. Control of the shunt connected reactive element is coordinated with the control of converters in order to supply the bulk of the total required reactive power.

The hybrid power flow controller is installed on a transmission path, so that, it is dividing the path into two transmission line segments. This is shown in Fig.1. The line to neutral voltage at the point of connection of the hybrid power flow controller with one line segment has been denoted by  $V_1$ . The voltage at the point of connection of the other line segment to the HPFC has been denoted by  $V_2$ . The three-phase transmission line segments are carrying three-phase alternating currents denoted by  $I_S$  and  $I_R$  as shown in Fig.2. The voltage sources  $V_X$  and  $V_Y$  represent the high voltage equivalents of the voltages generated by the voltage source converters  $VSC_X$  and  $VSC_Y$  respectively.  $B_M$  represents the controllable shunt connected variable susceptance. Active and reactive powers of converters have been denoted by  $P_X$ ,  $Q_X$ ,  $P_Y$ , and  $Q_Y$  respectively.

Switching functions have been approximated by their fundamental frequency components neglecting the harmonics. HPFC can be modeled by transforming the three-phase voltages and currents to dqo variables using Park's transformation. This is given by [11]:

$$V_{dqo} = T V_{abc} \quad (1)$$

$$\text{where } T = \frac{2}{3} \begin{pmatrix} \cos \theta & \cos (\theta - 120) & \cos (\theta + 120) \\ -\sin \theta & -\sin (\theta - 120) & -\sin (\theta + 120) \\ \frac{1}{\sqrt{2}} & \frac{1}{\sqrt{2}} & \frac{1}{\sqrt{2}} \end{pmatrix}$$

The two voltage source converters connected in series have been represented by controllable voltage sources  $V_X$  and  $V_Y$ . On the other hand,  $V_M$  is the voltage at the point where the variable susceptance is connected.  $L_R, L_S, R_R, R_S$  are the inductances and resistances of transmission line of both sides of HPFC.  $P_X$  is the real power exchange of the converter  $VSC_X$  with the dc link and  $P_Y$  is the real power exchange of the converter  $VSC_Y$  with the dc link. It is obvious that at any instant of time,

$$P_X = P_Y$$

The shunt connected variable susceptance or capacitance has been modeled by means of the differential equations given below:

$$\frac{B_M}{\omega} \frac{dV_{Md}}{dt} + B_M V_{Mq} = I_{Md} = I_{Sd} - I_{Rd} \quad (2)$$

$$\frac{B_M}{\omega} \frac{dV_{Mq}}{dt} + B_M V_{Md} = I_{Mq} = I_{Sq} - I_{Rq} \quad (3)$$

Model of the series converter  $VSC_X$  and the line segment on the sending end is given by:

$$L_S \frac{dI_{Sd}}{dt} + \omega L_S I_{Sq} + R_S I_{Sd} + V_{Xd} + V_{Md} = V_{Sd} \quad (4)$$

$$L_S \frac{dI_{Sq}}{dt} + \omega L_S I_{Sd} + R_S I_{Sq} + V_{Xq} + V_{Mq} = V_{Sq} \quad (5)$$

The differential equations describing the dynamics of the series converter  $VSC_Y$  and the line segment on the receiving end is given by:

$$L_R \frac{dI_{Rd}}{dt} + R_R I_{Rd} + V_{Rd} = V_{Md} + V_{Yd} + \omega L_R I_{Rq} \quad (6)$$

$$L_R \frac{dI_{Rq}}{dt} + R_R I_{Rq} + V_{Rq} = V_{Mq} + V_{Yq} + \omega L_R I_{Rd} \quad (7)$$

The differential equation describing the dynamics of  $V_{dc}$  is given by:

$$C_{dc} \frac{dV_{dc}}{dt} = \frac{1}{V_{dc}} (P_X - P_Y) \quad (8)$$

The dc circuit permits the exchange of active power between the converters. HPFC can be used to independently and simultaneously control the flow of active power through the line and the amounts of reactive power exchanged with the sending end and receiving end [12]. HPFC can thus be regarded as the functional equivalent of UPFC. The influence of HPFC on power system stability, mainly transient stability has been investigated in the following sections.

### III. MODELLING OF A MULTI-MACHINE SYSTEM USING LABVIEW

The popular Western System Coordinated Council (WSCC) 3-machines 9-bus practical power system with loads assumed to be represented by constant impedance model and all the three machines are operated with constant mechanical power input and with constant excitation has been considered as the test case. Fig.3 shows the WSCC 3-machines, 9-bus system. WSCC system is widely used and found very frequently in the relevant literature [13-14]. The base MVA of the system is 100, and system frequency is 60 Hz. The other data are given in Table 1 [4]. All time constants are in seconds. The disturbance, for the power system under study, initiating the transient has been considered as a three-phase fault occurring near bus number 7 at the end of the line 5-7.

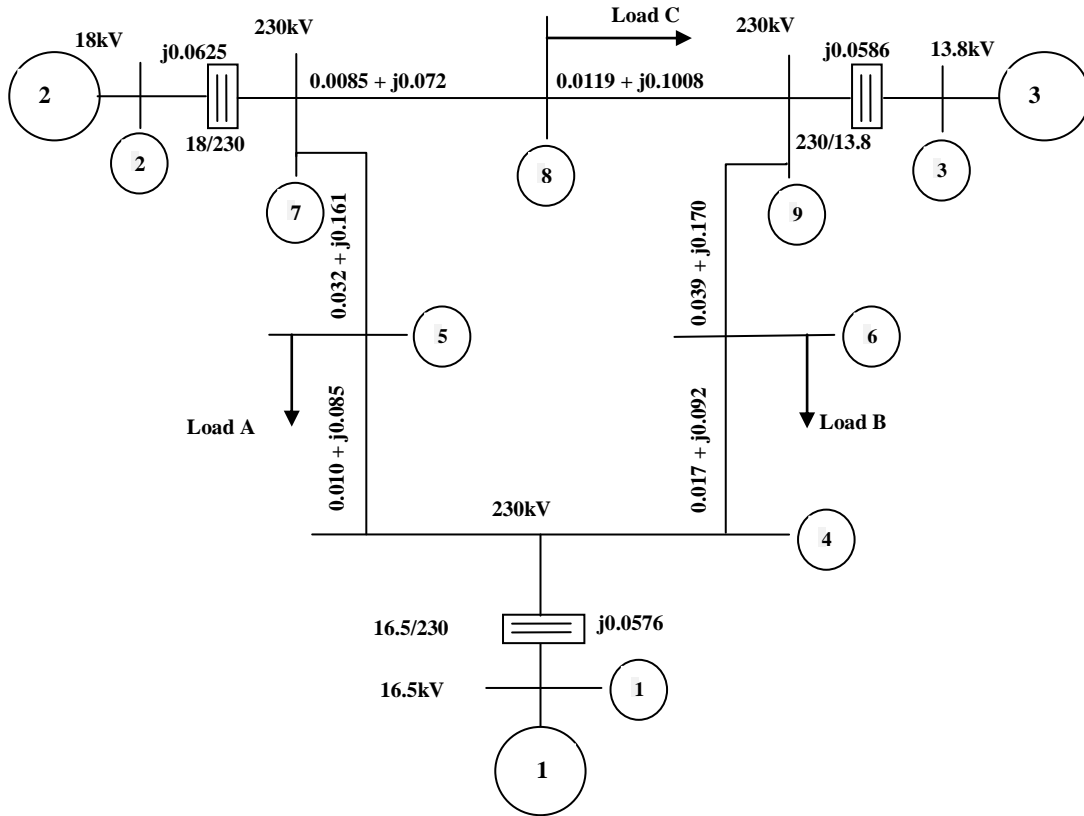


Fig.3 WSCC 3-Machines, 9-Bus System

Table 1 Generator-Data

Specifications	Generator 1	Generator 2	Generator 3
Rated MVA	247.5	192.0	128.0
kV	16.5	18.0	13.8
H(s)	23.64	6.4	3.01
Power factor	1.0	0.85	0.85
Type	Hydro	Steam	Steam
Speed	180 r/min.	3600 r/min.	3600 r/min.
$X_d$	0.1460	0.8958	1.3125
$X_d'$	0.0608	0.1198	0.1813
$X_q$	0.0969	0.8645	1.2578
$X_q'$	0.0969	0.1969	0.25
$X_l$ (leakage)	0.0336	0.0521	0.0742
$T_{do}$	8.96	6.00	5.89
$T_{qo}$	0	0.535	0.600
Stored energy at rated speed	2364 MWs	640 MWs	301 MWs

The resultant reduced Y matrices of the system before, and during the fault conditions are worked out and are given as  $Y_{Rpf}$  and  $Y_{Rdf}$  respectively.

Reduced Y matrix for the network in the pre-fault condition is given by:

$$Y_{Rpf} = \begin{bmatrix} 0.8455 - j2.9883 & 0.2871 + j1.5129 & 0.2096 + j1.2256 \\ 0.2871 + j1.5129 & 0.4200 - j2.7239 & 0.2133 + j1.0879 \\ 0.2096 + j1.2256 & 0.2133 + j1.0879 & 0.2770 - j2.3681 \end{bmatrix} \quad (9)$$

Reduced Y matrix for the network during-fault condition is similarly, given by:

$$Y_{Rdf} = \begin{matrix} 0.6568 \left\{ \begin{matrix} j3.8160 & 0 & 0.0701 + j0.6306 \\ 0 & 0 - j5.4855 & 0 \\ 0.0701 + j0.6306 & 0 & 0.1740 - j2.7959 \end{matrix} \right\} \end{matrix} \quad (10)$$

The WSCC 3-machines 9-bus system has been modelled using LabVIEW and considered as the test case for the transient stability enhancement investigations carried out in the following sections.

LabVIEW is a very powerful and flexible tool. It is basically a software package having provision of environment for graphical development. LabVIEW enables simulation of instrumentation schemes and their analyses. LabVIEW has features regarding built-in virtual instrument modules and can thus, provide a graphical environment for simulation. It can produce a visual representation of the system. The software has a huge potential for analyzing system performance and can be used in simulation techniques effectively.

LabVIEW consists of a variety of tools for analysis including built-in-functions and add-on-toolkits. LabVIEW now has several toolkits and modules in the areas of control and simulation, signal processing, system identification, mathematics etc. The LabVIEW Control and Simulations Toolkit (Module) contains a block diagram based environment for simulation of linear and non-linear continuous-time and discrete-time dynamic systems. Many simulation algorithms such as various Runge-Kutta methods are available. The mathematical model to be simulated must be represented in a simulation loop which is similar to an ordinary while loop in LabVIEW. The mathematical models of the SMIB Electrical power systems with and without incorporating the different FACTS controllers have been simulated, using the LabVIEW Control and Simulation Toolkit.

#### IV. MODELLING OF MULTI-MACHINE SYSTEM EQUIPPED WITH HPFC1

The topology of HPFC proposed by Bebic et al [9] as shown in Fig.1 have been simulated using LabVIEW software. Two configurations of HPFC have been modeled and simulated using LabVIEW. The control performance of these topologies has been investigated and analyzed. These are discussed in the following sections:

The first configuration of HPFC, termed as HPFC1, has been simulated as a combination of two VSCs in series and one shunt capacitor. The middle shunt element has been substituted by a presumably existing switched capacitor or SVC, with the two half-sized series converters. The transfer function models for the series converters and the SVC have been combined together to form the LabVIEW model of HPFC1. The LabVIEW based model of HPFC1, which is a combination of series converters or SSSC and SVC, has been simulated as shown in Fig.4. The HPFC model simulated as shown in Fig.4 has been implemented in the MM system as shown in Fig.5.

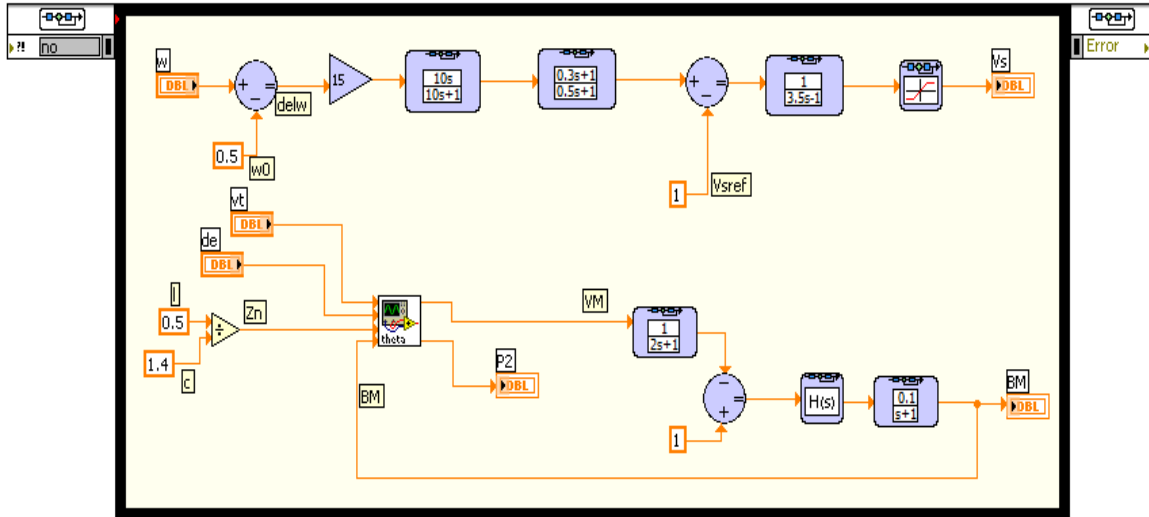


Fig.4. LabVIEW Based Model of HPFC1

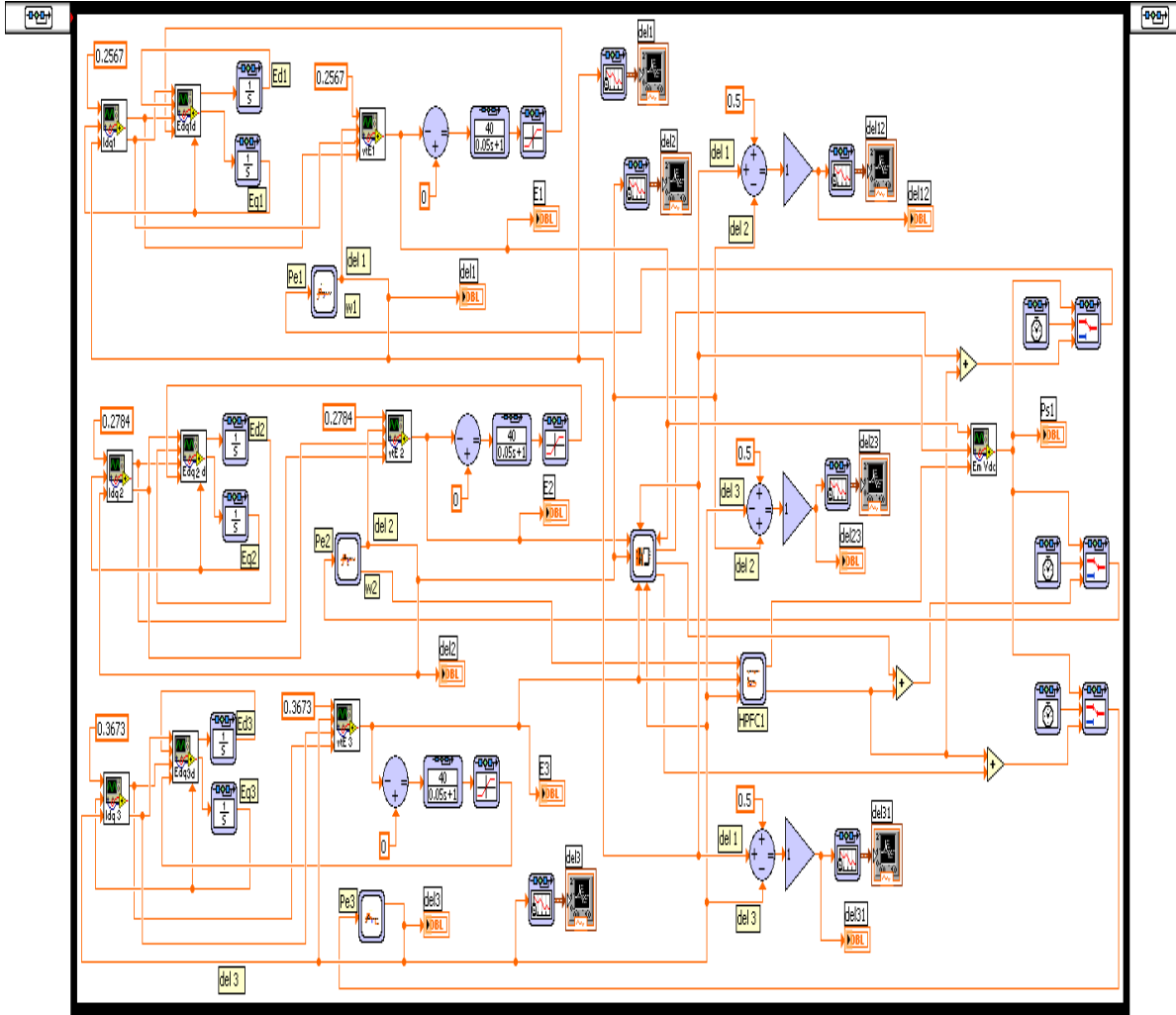


Fig.5 LabVIEW Based Model of MM Power System Equipped with HPFC1

The controller consists of amplification block, a wash-out block with low pass filters and stages of lead-lag blocks. The parameters of the HPFC are as under:

Measurement time constant, $T_m = 2$ ,	Gain of voltage regulator block, $K_R = 0.2$ ,
Time constant of voltage regulator block, $T_R = 0.7$ ,	Thyristor dead time, $T_d = 0.0016$ ,
Thyristor firing delay time, $T_b = 1$	Controller gain, $K = 15$ ,
Wash-out time constant, $T_w = 10$ ,	
Lead-lag time constant of different stages: $T_{1s} = 0.3$	$T_{2s} = 0.5$ $T_{3s} = 3.5$

In order to analyze the ability of the controller to stabilize the system under study, the disturbance initiating the transient has been considered as a three-phase fault occurring near bus no.7 at the end of the line 5-7.

Fig.5 shows the LabVIEW based model of Multi-Machine system equipped with HPFC1. The main objective of transient stability simulation of power system is to investigate and analyze the stability of a power system over a time period from few seconds to several tens of seconds, plotting the response of generator rotor-angle with time. Values of damping constant of machine1 ( $D_1$ ), machine2 ( $D_2$ ) and machine3 ( $D_3$ ) have been varied and system stability has been investigated by plotting relative angular positions versus time curves. While varying the values of damping constant  $D_1$ ,  $D_2$  and  $D_3$ , they are kept equal at each instant. Fig.6 shows the variation of relative angular positions with time for the 3 machines 9-bus system equipped with HPFC1 corresponding to the damping constant values  $D_1 = D_2 = D_3 = 10$ .

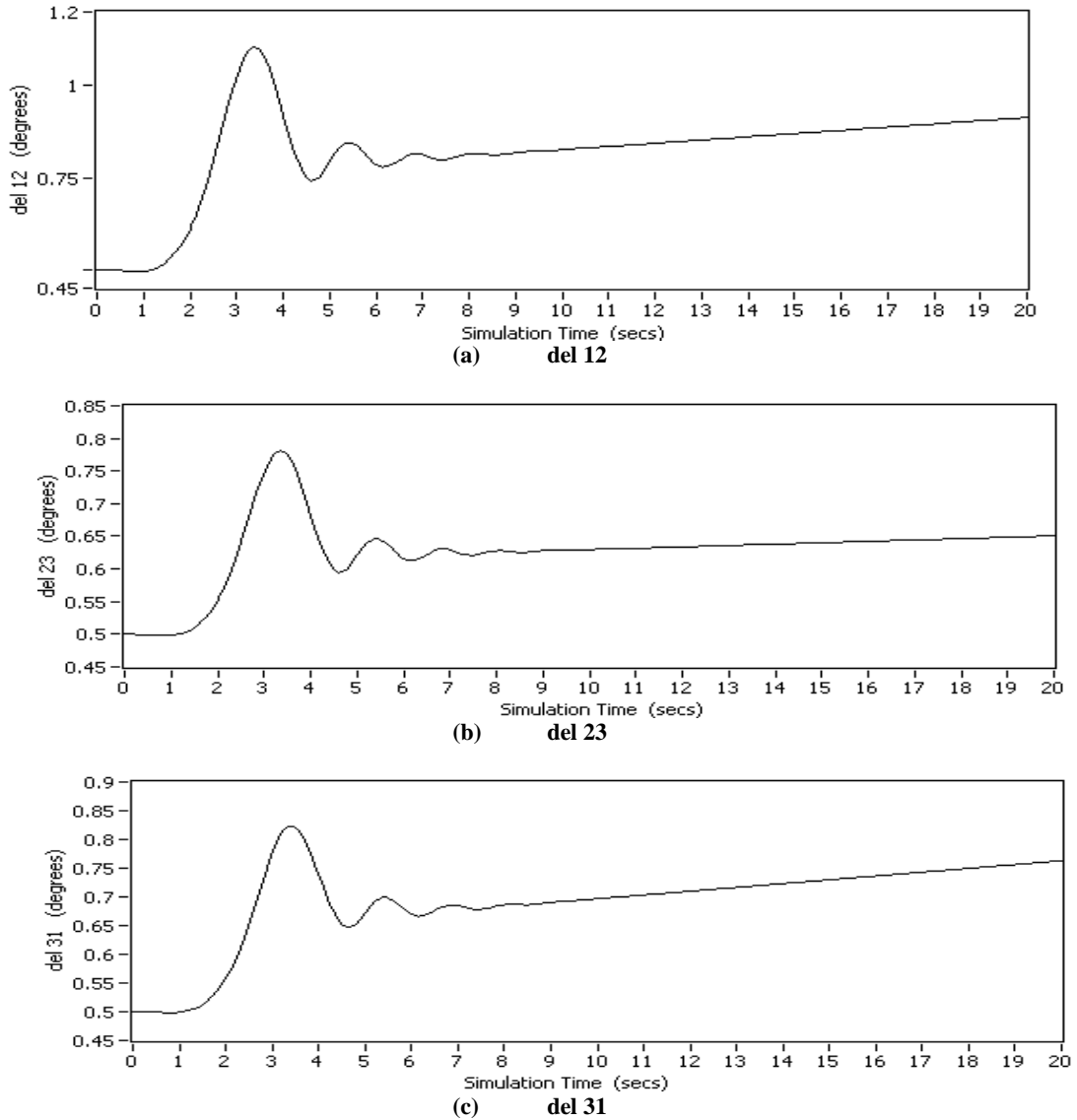


**Fig. 6** Variation of Relative Angular Positions: del 12, del 23 and del 31, with Time, for  $D_1 = D_2 = D_3 = 10$  in case of MM System Equipped with HPFC1

Table 2 indicates the steady state stable values, the time taken to attain stability, the maximum value of overshoot and the value of rise-time of relative angular positions: del12, del23 and del31 when the values of damping constant  $D_1, D_2, D_3$  are varied. As the values of damping constant are increased, the oscillations start reducing, the time taken to attain stability and the maximum value of overshoot reduce.

**Table 2** Steady State Stable Values, Value of Time Taken to Attain Stability, Maximum Value of Overshoot and Value of Rise Time of Relative Angular Positions: del 12, del 23 and del 31, with Varying Values of Damping Constant  $D_1, D_2$  and  $D_3$  for a 3 Machines 9 Bus System Equipped with HPFC1

Value of Damping Constants ( $D_1=D_2=D_3$ )	Stable Value of Relative Angular Positions (degrees)			Value of Time Taken to Attain Stability (seconds)			Maximum Value of Overshoot (degrees)			Value of Rise Time (seconds)		
	del 12	del 23	del 31	del 12	del 23	del 31	del 12	del 23	del 31	del 12	del 23	del 31
0	unstable											
1	System goes on diverging, not attaining a steady state						First swing is not the maximum overshoot, subsequent oscillations also goes diverging					
2	System goes on diverging, not attaining a steady state						1.49	1.42	2.4	4.9	4.8	4.8
3	2.0	1.32	2.75	21.5	22	21	1.4	1.33	2.23	4.7	4.6	4.7
4	1.6	1.13	2.25	19.5	20	19.5	1.34	1.27	2.1	4.6	4.5	4.5

5	1.4	1.0	1.9	17	18	17.5	1.28	1.21	1.99	4.5	4.4	4.4
8	1.06	0.81	1.39	15.5	16	15.5	1.16	1.09	1.75	4.4	4.3	4.3
10	0.95	0.75	1.2	14.5	14.5	15	1.10	1.03	1.63	4.3	4.2	4.3
15	0.79	0.67	0.97	13	13.5	13	0.99	0.92	1.41	4.2	4.1	4.2
20	0.72	0.63	0.85	13.5	12.5	13	0.91	0.84	1.25	4.2	4.1	4.2
25	0.68	0.6	0.78	10.5	11	11	0.86	0.78	1.13	4.2	4.2	4.2
30	0.65	0.58	0.73	10	11	10.5	0.8	0.74	1.04	4.3	4.2	4.3
35	0.63	0.57	0.69	8.5	10	9.5	0.76	0.71	0.97	4.3	4.3	4.3
40	0.61	0.56	0.67	8.5	9	9	0.74	0.69	0.92	4.4	4.3	4.4
45	0.59	0.56	0.65	8.5	9	9.5	0.71	0.66	0.88	4.4	4.3	4.4
50	0.59	0.55	0.64	8	8.5	8.5	0.69	0.65	0.84	4.5	4.4	4.5

**V. MODELLING OF MULTI-MACHINE SYSTEM EQUIPPED WITH HPFC2**

The previous configuration of HPFC, termed as HPFC1, employed transfer function models of SVC and series converters (SSSC). It is apparent that the functional equivalents of an SVC, such as a mechanically switched compensator bank, or a STATCOM or a synchronous condenser can be successfully employed.

The investigator envisaged to design another model using the above principle by replacing the SVC with a STATCOM. The transfer function models for the series converters and the STATCOM have been combined together to form the LabVIEW model of HPFC2.

The LabVIEW based model of HPFC2, which is a combination of series converters or SSSC and STATCOM, has been simulated as shown in Fig.7.

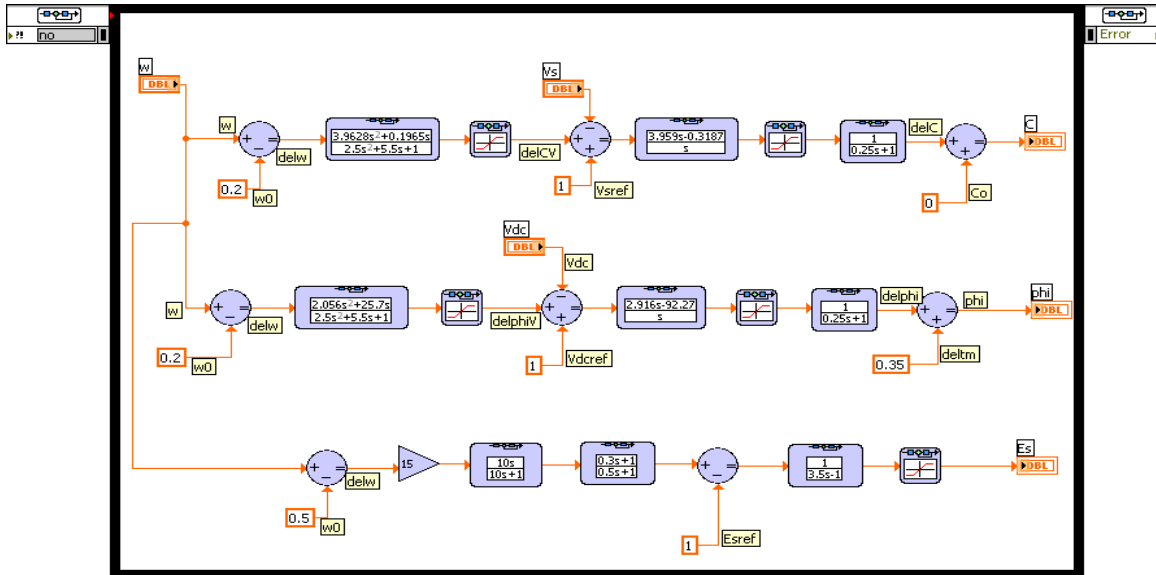


Fig.7 LabVIEW based Model of HPFC2

The parameters of HPFC2 are as under:

Controller gain,  $K=15$ ,

Wash-out time constant,  $T_w=10$ ,

Lead-lag time constant of different stages:  $T_{1s}=0.3T_{2s}=0.5$       $T_{ss}=3.5$

AC and DC voltage stabilizer gains,  $K_C = 3.91$ ,      $K_\phi = 51.4$ ,

Lead-lag damping stabilizer time constants,  $T_{1C} = 0.305s$ ,      $T_{2C} = 0.5s$ ,

Lead-lag damping stabilizer time constants,  $T_{1\phi} = 0.008s$ ,      $T_{2\phi} = 0.5s$ ,

AC voltage PI controller gains,  $K_{P,ac} = 5.959$ ,      $K_{I,ac} = -31.87$

DC voltage PI controller gains,  $K_{P,dc} = 2.916$ ,      $K_{I,dc} = -92.27$ ,

$K_F = 1.0$ ,  $T_F = 0.25s$ .

The second configuration of HPFC termed as HPFC2 has been simulated and the LabVIEW based model of HPFC2 is shown in Fig.7. The LabVIEW based model of 3-Machine 9 bus WSCC system equipped with HPFC2 is almost similar to as shown in Fig.5. Values of damping constant of machine1 ( $D_1$ ), machine2 ( $D_2$ ) and machine3 ( $D_3$ ) have been varied and system stability has been investigated. Fig.8 shows the variation of relative angular positions with time for the 3 machines 9-bus system equipped with HPFC2 corresponding to the damping constant values  $D_1, D_2, D_3$  equal to 10. The system attains stability faster when the damping constant is increased. The oscillations die out completely. This is clearly seen in Fig.8. For a damping constant value equal to 0, the system becomes unstable. The system behaves almost different when the value of damping constant equal to 1 or 2. The system oscillations die out but the system does not attain a stable value. The stable value goes on increasing.

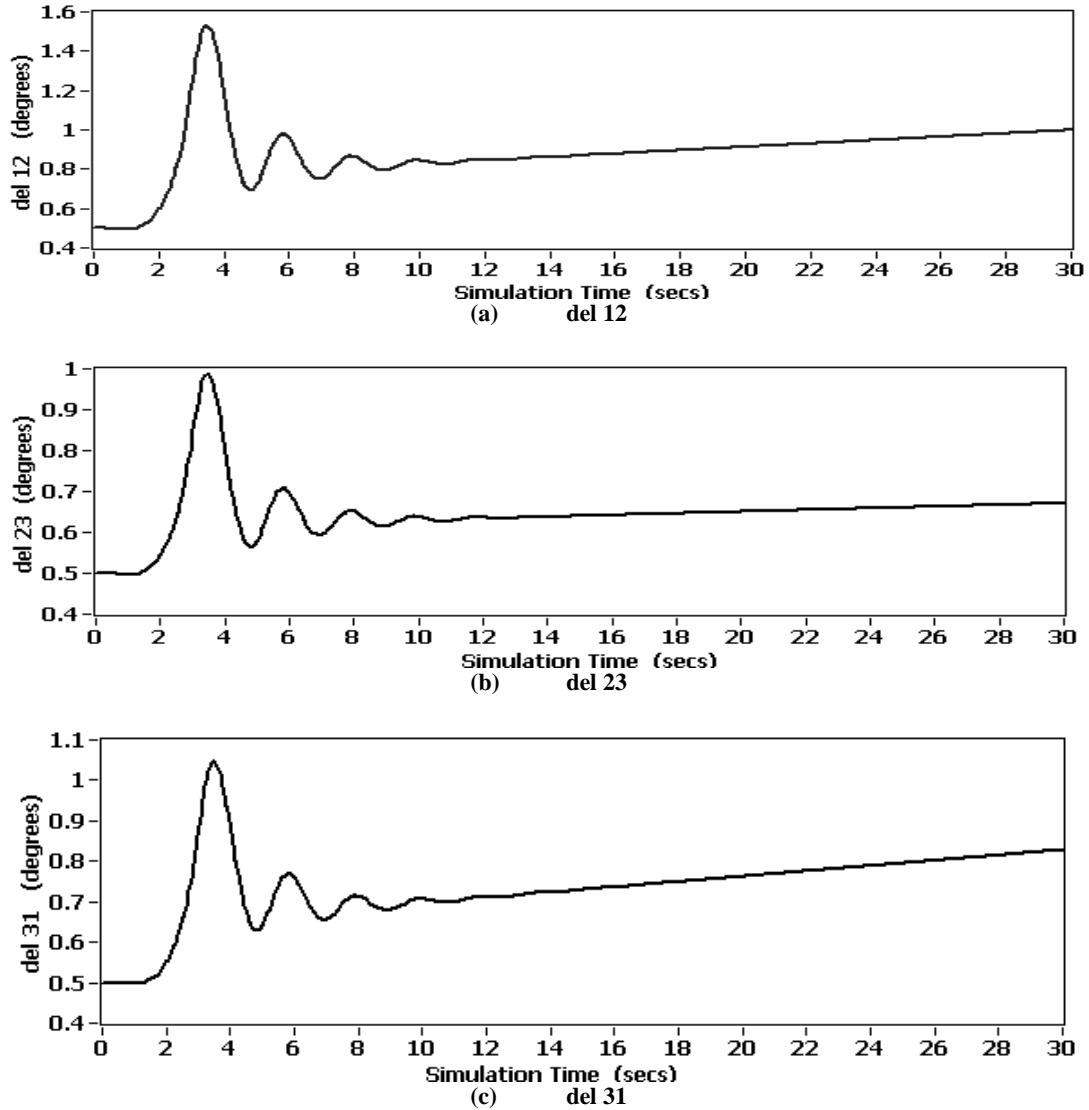


Fig. 8 Variation of Relative Angular Positions: del 12, del 23 and del 31, with Time, for  $D_1 = D_2 = D_3 = 10$  In case of MM System Equipped with HPFC2

The steady state stable values, the time taken to attain stability, the maximum value of overshoot and the value of rise-time of relative angular positions: del12, del23 and del31 for varying values of damping constants  $D_1, D_2, D_3$ , have been observed and the values are similar to those in Table 2. It is observed that the steady state stable values, the time taken to attain stability, and the maximum value of overshoot of relative angular positions: del12, del23 and del31 decreases when the values of damping constant  $D_1, D_2, D_3$  are increased.

## VI. MODELLING OF A THIRD CONFIGURATION OF HPFC

Out of the two HPFC topologies proposed by Bebic et al, the first one is shown in Fig.1. The second topology is a dual of the first. This topology can be obtained by following a simple circuit transformation of the one shown in Fig.1. This topology is shown in Fig.9(a) and (b). In Fig.9(a) voltage sources  $V_X$  and  $V_Y$  represent the high voltage equivalents of voltages generated by the voltage source converters  $VSC_X$  and  $VSC_Y$  respectively. It is assumed that the shunt connected variable susceptance  $B_M$  is replaced by a shunt connected current source  $I_M$  as shown in Fig.9(a). It is also assumed that the current source is split into two half-value currents  $I_{M1}$  and  $I_{M2}$ . The two voltage sources are assumed to be combined into one as  $V_X - V_Y$  as shown in Fig.9(b). Finally let the series connected voltage source be regarded as a variable reactance and the shunt connected current sources as shunt connected voltage source converters. As in the case of the original circuit, the converters couple each other's dc terminals, and hence, are able to exchange active power between each other. This topological variation of the HPFC can be used to improve the performance of the series capacitors by connecting shunt connected voltage source converters. Both topologies make combined use of passive components and converters and can therefore be regarded as hybrid devices. The above discussed topology can be envisioned in an SMIB power system as shown in Fig.10.

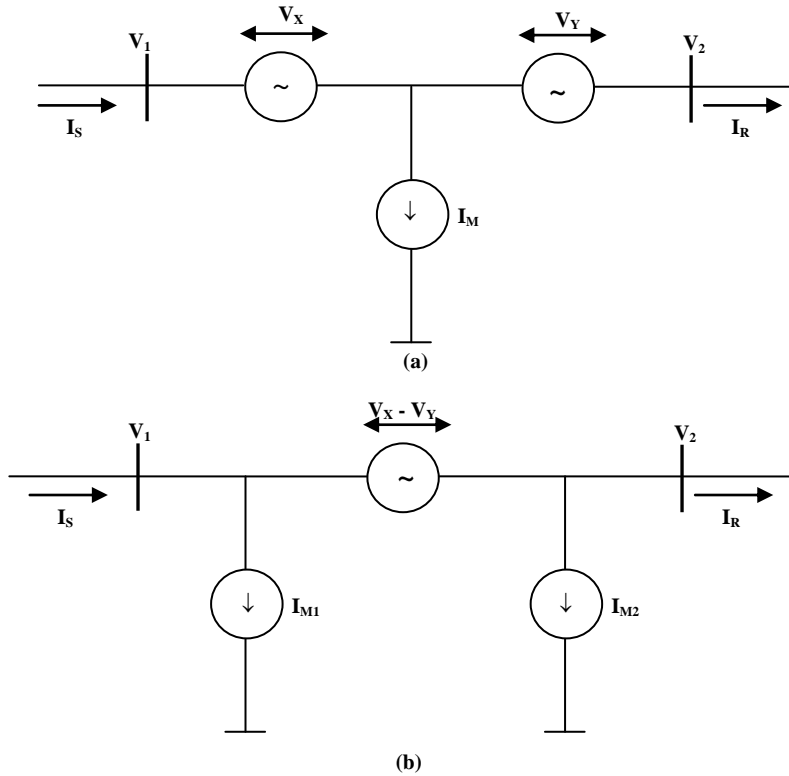


Fig.9 HPFC – Circuit Transformations (a) Equivalent of the First Topology, (b) Rearranged Equivalent

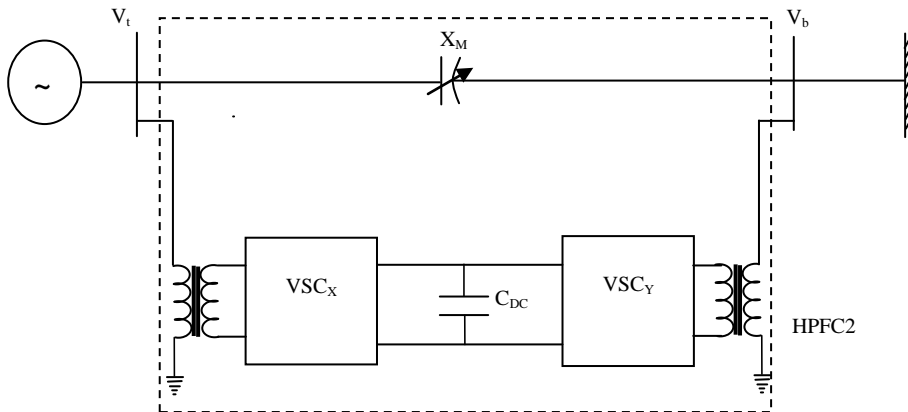


Fig.10 SMIB Power System Equipped with an HPFC (Second Topology)

The second topology of HPFC, shown in Fig.10, can be simulated as a combination of two VSCs connected in shunt with one series connected capacitor. The middle series element has been substituted by a presumably existing switched capacitor or TCSC, with the two half-sized shunt converters. This configuration is termed as HPFC3. The transfer function models of the shunt converters and the TCSC have been combined together to form the LabVIEW based model of HPFC3. The HPFC3 which is a combination of shunt converters or STATCOM and TCSC have been simulated and the LabVIEW based model of HPFC3 is as shown in Fig.11.

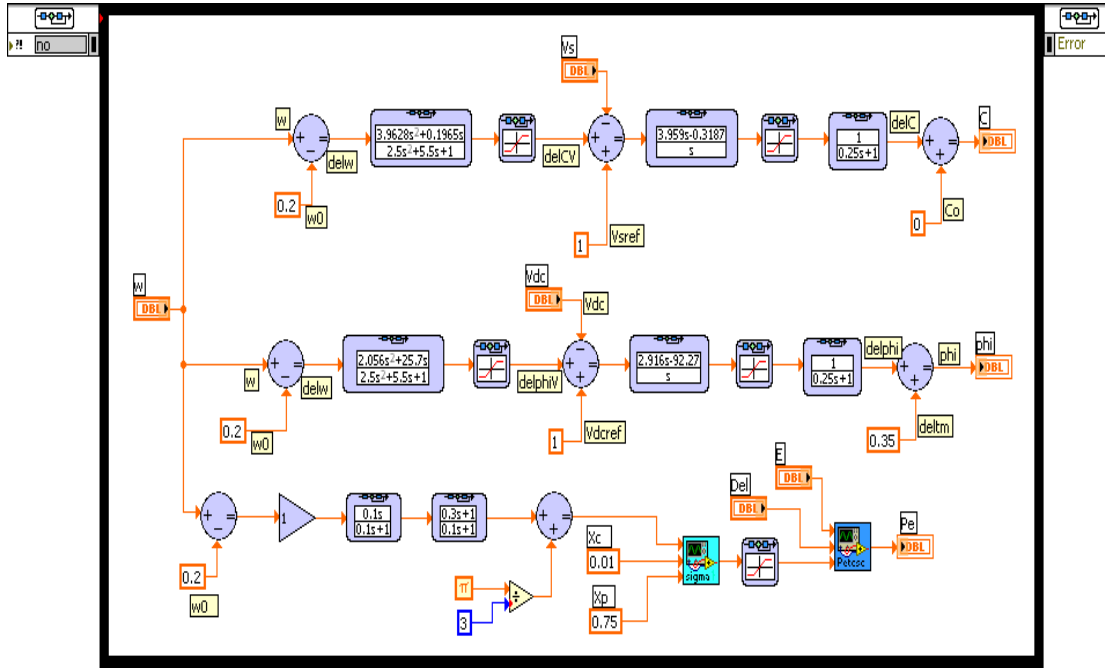


Fig.11 LabVIEW based Model of the HPFC3

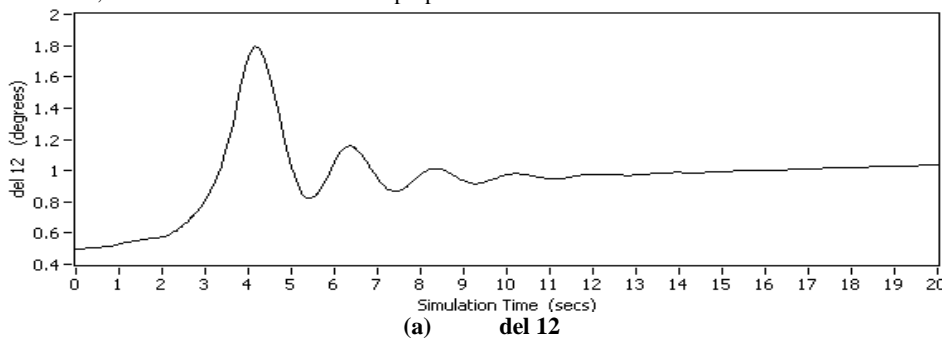
The parameters of HPFC3 are as under:

- Block gain,  $K = 20$ ,
- Wash out block time constant,  $T_w = 0.1$ ,
- Lead-lag block time constants,  $T_1 = 0.4$  and  $T_2 = 0.5$ ,
- Nominal reactance of the fixed series capacitor,  $X_c = 0.01$ ,
- Reactance of the inductor connected in parallel to the capacitor,  $X_p = 0.75$ .
- AC and DC voltage stabilizer gains,  $K_C = 3.91$ ,  $K_\phi = 51.4$ ,
- Lead-lag damping stabilizer time constants,  $T_{1C} = 0.305s$ ,  $T_{2C} = 0.5s$ ,
- Lead-lag damping stabilizer time constants,  $T_{1\phi} = 0.008s$ ,  $T_{2\phi} = 0.5s$ ,
- AC voltage PI controller gains,  $K_{P,ac} = 5.959$ ,  $K_{I,ac} = -31.87$
- DC voltage PI controller gains,  $K_{P,dc} = 2.916$ ,  $K_{I,dc} = -92.27$ ,
- $K_F = 1.0$ ,  $T_F = 0.25s$ .

The model of HPFC3 simulated as shown in Fig.11, has been incorporated in a 3-Machine 9 bus WSCC system and has been investigated for transient stability enhancements. Values of damping constant of machine1 ( $D_1$ ), machine2 ( $D_2$ ) and machine3 ( $D_3$ ) have been varied and system stability has been investigated. Fig.12 shows the variation of relative angular positions with time for the 3 machines 9-bus system equipped with HPFC3 corresponding to the damping constant values  $D_1, D_2, D_3$  equal to 10. The steady state stable values, the time taken to attain stability, the maximum value of overshoot and the value of rise-time of relative angular positions: del12, del23 and del31 for varying values of damping constants  $D_1, D_2, D_3$ , have been tabulated in Table 3.

It is observed that the system behaves almost in the similar manner with all the three configurations of HPFC. This is established by comparing Tables 2 and 3.

It is clearly observed that Fig.8 is very much similar to Fig.12. It is also seen that the values in Tables 2 and 3 are almost the same. The performance characteristics of HPFC1, HPFC2 and HPFC3 are very much similar and all the three configurations of HPFC can be implemented as a FACTS controller in a multi-machine system. A comparative chart comparing the values of time taken to attain stability of the 3 machines 9 bus system when equipped with any of the three configurations HPFC1, HPFC2 and HPFC3 has been prepared and is shown in Table 4.



(a) del 12

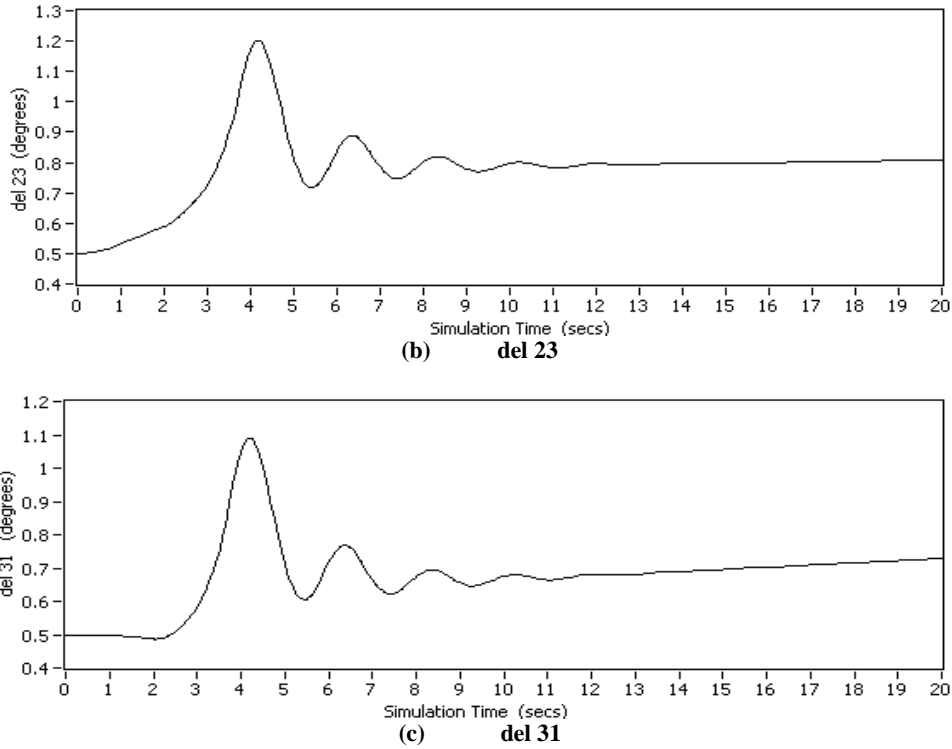


Fig.12 Variation of Relative Angular Positions: del 12, del 23 and del 31, with Time, for  $D_1 = D_2 = D_3 = 10$  in case of MM System Equipped with HPFC3

Table 3 Steady State Stable Values, Value of Time Taken to Attain Stability, Maximum Value of Overshoot and Value of Rise Time of Relative Angular Positions: del 12, del 23 and del 31, with Varying Values of Damping Constant  $D_1$ ,  $D_2$  and  $D_3$  for a 3 Machines 9 Bus System Equipped with HPFC3

Value of Damping Constants ( $D_1 = D_2 = D_3$ )	Stable Value of Relative Angular Positions (degrees)			Value of Time Taken to Attain Stability (seconds)			Maximum Value of Overshoot (degrees)			Value of Rise Time (seconds)		
	del 12	del 23	del 31	del 12	del 23	del 31	del 12	del 23	del 31	del 12	del 23	del 31
0	unstable											
1	System goes on diverging, oscillations die out but the value is diverging						First swing is not the maximum overshoot, subsequent peaks are also diverging					
2	System goes on diverging, oscillations die out but the value is diverging						3.4	2.2	1.8	4.7	4.6	4.7
3	3.2	1.8	1.75	39	38	37	3.2	2.0	1.7	4.5	4.6	4.6
4	2.3	1.4	1.4	29	30	27	3.0	1.9	1.7	4.5	4.5	4.5
5	1.9	1.3	1.2	25	26	27	2.9	1.7	1.6	4.5	4.4	4.5
8	1.35	0.96	0.88	19	18	19	2.46	1.54	1.44	4.4	4.4	4.4
10	1.15	0.86	0.8	13	13.5	12.5	2.26	1.43	1.35	4.4	4.4	4.4
15	0.93	0.74	0.68	11	11.5	11.5	1.9	1.21	1.19	4.5	4.4	4.5
20	0.81	0.68	0.63	9	9.5	9	1.64	1.08	1.07	4.6	4.6	4.6
25	0.75	0.64	0.61	8.5	8.5	9	1.45	0.97	0.99	4.7	4.7	4.8
30	0.71	0.62	0.59	8.5	9	8.5	1.32	0.9	0.92	5.0	5.0	5.0
35	0.68	0.6	0.57	8	8.5	8	1.21	0.85	0.87	5.3	5.3	5.3
40	0.65	0.58	0.56	8	8.5	8	1.14	0.81	0.83	5.9	5.9	5.9
45	0.6	0.57	0.54	8	8.5	8	0.88	0.69	0.69	6.3	6.3	6.3
50	0.58	0.56	0.55	8	8	8	0.86	0.68	0.65	6.4	6.3	6.4

**Table 4** Comparative Chart Combining Values of Time Taken to Attain Stability of Relative Angular Positions: del 12, del 23 and del 31, for HPFC1, HPFC2 and HPFC3 with Varying Values of Damping Constants  $D_1, D_2$  and  $D_3$  for a 3 Machines 9 Bus System

Value of Damping Constants ( $D_1=D_2=D_3$ )	HPFC1			HPFC2			HPFC3		
	del 12	del 23	del 31	del 12	del 23	del 31	del 12	del 23	del 31
0	unstable			unstable			unstable		
1	Oscillations die out, but stable value goes on increasing			Oscillations die out, but stable value goes on increasing			Oscillations die out, but stable value goes on increasing		
2									
3	21.5	22	21	33	35	32	39	38	37
4	19.5	20	19.5	28	28	24	29	30	27
5	17	18	17.5	22	22	20	25	26	27
8	15.5	16	15.5	15	15	13	19	18	19
10	14.5	14.5	15	13	13	12	13	13.5	12.5
15	13	13.5	13	11	11	10	11	11.5	11.5
20	13.5	12.5	13	9	9	9	9	9.5	9
25	10.5	11	11	8	8	8	8.5	8.5	9
30	10	11	10.5	7	7	7	8.5	9	8.5
35	8.5	10	9.5	7	7	7	8	8.5	8
40	8.5	9	9	6	6	6	8	8.5	8
45	8.5	9	9.5	6	6	6	8	8.5	8
50	8	8.5	8.5	6	6	6	8	8	8

It is clearly seen that the system behaves almost in the same manner. For a value of damping constant equal to 0, the system becomes unstable. When the damping constant is increased to 1 or 2, the system oscillations die out but it does not attain a constant stable value. The stable value goes on increasing. For increasing values of damping constant, the settling time improves considerably. This shows that HPFC is effective in improving stability.

## VII. CONCLUSION

The goal of transient stability simulation of power systems is to analyze the stability of a power system. A power system is deemed to be stable if the rotational speeds of the generators return to their normal values in a quick and stable manner after a sudden fault. Three configurations of HPFC viz. HPFC1, HPFC2 and HPFC3 have been modeled and simulated using LabVIEW and the control performance of these controllers when incorporated in a 3 machines, 9 bus system, in terms of transient stability enhancement, has been investigated and analyzed in the present work. The transfer function models for the series converters, SVC, TCSC and the STATCOM have been employed to form the LabVIEW models of HPFC1, HPFC2 and HPFC3. Variations of the relative angular positions of generators with time has thus been plotted and the steady-state stable-values, time taken to attain stability, the maximum value of overshoot and the rise-time have been found out in each case and tabulated for comparison purposes. It is clearly observed from the comparative analysis that the dynamic performance of the power system has quite a bit improved with the HPFC. All the three HPFC configurations behave almost in the similar manner. The value of time taken to attain stability starts reducing drastically with increase in the value of damping constant. It is also observed that the maximum value of overshoot decreases and the value of rise-time increases slightly with the increase in the value of damping constant. It is evident from the simulation results that all the three configurations can be utilised effectively as a controller in the system for damping out system oscillations.

Encouraging results have been obtained which shows that HPFC is very effective in improving stability. Another major benefit of the new topology ie. HPFC is, that it is capable of fully utilizing the existing equipment (switched capacitors or SVC) and thereby the required ratings of the additional converters are substantially lower as compared to the ratings of the comparable UPFC model.

## REFERENCES

- [1]. Masood T., Edris A.A, Aggarwal RK, Qureshi.S.A., Khan.A.J., Yacob.Y.A, "Static VAR Compensator (SVC) Modeling and Analysis Techniques by MATLAB", Power System Conference PSC 2006, pp.1-7, 2006.
- [2]. Lee.S.Y, Bhattacharya.S, Lejonberg.T, Hammad.A, Lefebvre.S, "Detailed Modeling of Static VAR Compensators using the Electromagnetic Transients Program (EMTP)", IEEE Transactions On Power Delivery, Vol. 7. No. 2, pp. 836-847, 1992.
- [3]. Juncheng.G, Luyuan.T, Jun.G, Zhonghong.W., " Mathematical Model for Describing Characteristics of TCSC", Proceedings of the International Conference Power System Technology PowerCon 2002, Vol.3, pp.1498-1502, 2002.
- [4]. Patel.R, Mahajan.V, Pant.V, "Modelling of TCSC Controller for Transient Stability Enhancement", International Journal of Emerging Electric Power Systems, Vol.7, Issue.1, Article.6, pp. 1-17, 2006.
- [5]. Taheri.H, Shahabi.S, Taheri.Sh, Gholami.A, "Application of Synchronous Static Series Compensator (SSSC) on Enhancement of Voltage Stability and Power Oscillation Damping", Proceedings of the IEEE Region 8 Conference, EUROCON 2009, pp.533-539, 2009.

- [6]. Panda.S, “Modelling, Simulation and Optimal Tuning of SSSC-based Controller in a Multi-Machine Power System”, World Journal of Modelling and Simulation, Vol.6, No.2, pp. 110-121, 2010.
- [7]. Abido.M.A, Weindl.Ch, Herold.G, “Analysis and Assessment of STATCOM based Damping Stabilizers for Power System Stability Enhancement”, Science Direct Journal of Electric Power Systems Research, Vol.73, No.2, pp.177-185, Feb. 2005.
- [8]. Fawzi.A.R.A.J., “Analysis of Damping Torque and Synchronising Torque Contributed by STATCOM Considering Two Different Damping Schemes”, International Journal of Emerging Electric Power Systems, Vol.12, Issue 2, Article 3, 2011.
- [9]. Bebic.J.Z., “The Hybrid Power Flow Controller - Introduction to HPFC”, 2007, Available at <http://www.hpfc.ca/hpfc.html>
- [10]. Bebic.J.Z., Lehn.P.W., Iravani.M.R., “The Hybrid Power Flow Controller - A New Concept for Flexible AC Transmission”, Proceedings of the IEEE Power Engineering Society General Meeting, pp.1-7, 2006.
- [11]. Rakesh Babu.G., Bhargav.K.V., Rambabu, “Real and Reactive Power Control of HPFC with Adaptive Back Stepping Control”, International Journal of Engineering Science and Technology, Vol.3, No.5, May 2011.
- [12]. Sood.V.K., Sivadas.S.D., “Simulation of Hybrid Power Flow Controller”, Proceedings of the Joint International Conference on Power Electronics, Drives and Energy Systems (PEDES) & Power India, pp.1-5, December 2010.
- [13]. Jyothsna.T.R, Vaisakh.K, “Improving Multi-Machine Transient Stability Using a Non- Linear Power System Stabilizer under Different Operating Conditions”, Fifteenth National Power Systems Conference (NPSC), pp.101-106, December, 2008.
- [14]. Patel.R, Bhatti T. S Kothari D. P, “MATLAB/ Simulink based Transient Stability Analysis of a Multi-Machine Power System”, International Journal of Electrical Engineering Education, Vol. 39, Issue 4, pp 320-336, October, 2002